ELSEVIER

Materials Chemistry and Physics 74 (2002) 98–103

MATERIALS CHEMISTRY AND PHYSICS

www.elsevier.com/locate/matchemphys

Plasticizer effect on the ionic conductivity of PEO-based polymer electrolyte

Xinming Qian, Ningyu Gu, Zhiliang Cheng, Xiurong Yang, Erkang Wang, Shaojun Dong*

Laboratory of Electroanalytical Chemistry, Changchun Institute of Applied Chemistry, Chinese Academy of Sciences, Jilin, Changchun 130022, PR China

Received 21 December 2000; received in revised form 20 April 2001; accepted 23 May 2001

Abstract

The effects of plasticizer ethylene carbonate (EC) on the AC impedance spectra and the ionic conductivity are reported. With increasing of EC concentration the semicircle in high frequency disappears, and the slope of the straight line in low frequency decreases. The data obtained from impedance experiments can be explained using an equivalent circuit proposed. On the other hand, the room temperature conductivity increases with EC concentration because of the increase of the segmental flexibility of PEO. For lower EC concentration samples, the temperature dependence of conductivity in low temperature range follows Arrhenius type, but when EC concentration is larger than 20%, the temperature dependence of conductivity obeys the Vogel–Tamman–Fulcher (VTF) equation in all temperature ranges.

Keywords: Poly(ethylene oxide) (PEO); Ethylene carbonate (EC); Ionic conductivity; Polymeric electrolyte; Impedance spectra

1. Introduction

Polymeric electrolytes have attracted considerable interest during the past few years, because of their potentially wide range of applications in such fields as fuel cells, rechargeable lithium batteries, electrochromic devices and sensors [1–3]. The advantages of using these solid polymeric electrolyte (SPE) are concentrated on their desirable characteristics: good compatibility with lithium metal; no leakage; low self-discharge in batteries; relax elastically under stress; easy processing and continuous production and so on [4,5]. However, the low ionic conductivity of SPE limits their applications. It has been recognized that the ionic transport of SPE occurs only in the amorphous polymer regions and is often governed by the segmental motion of polymer chain [6,7]. It is clear that the presence of a flexible, amorphous phase in SPE is essential for higher ionic conductivity. Even though the SPE study has been under development for over 20 years since Wright and coworkers [8] firstly reported in 1973, SPE technology is not yet commercialized [9]. A number of reviews have been published over the past few years [10–14].

Although many kinds of polymeric electrolytes such as poly(acrylonitrile) [15], poly(propylene oxide) [16], poly(methyl methacrylate) [17] and poly(maleic anhydride–styrene) [18] etc. based SPE have been studied, high molecular weight PEO-based SPE is still the most widely investigated system both for technological application and for fundamental studies [4,19]. The main drawback, however, is the low room temperature ionic conductivity due to the high crystalline fraction in PEO-based complexes. Several methods have been proposed to decrease the degree of crystallinity. The formation of cross-linked networks [20], block or com branch copolymers [1,21] and the composite SPE by the addition of organic, inorganic fillers or some plasticizers [6,7,15] are often used. Compared to the other methods, plasticization is the effective way to improve the conductivity of PEO-based SPE. Among a number of plasticizers, the most used plasticizers are low molecular weight organic solvents such as propylene carbonate (PC), ethylene carbonate (EC), dimethyl carbonate (DMC) and diethyl carbonate (DEC), etc. [22].

Many PEO-plasticizer systems have been studied using the above plasticizers. But previous reports are commonly focused on ionic conductivity, viscosity and the interactions among the components [23,24]. Although the AC impedance technique is used as the standard method to determine the ionic conductivity in literatures [1,10,25], the effects of plasticizer on the impedance spectra and the ion transport mechanism are scarcely studied. In the present work, an ion-conducting plasticized SPE based on PEO was prepared, in which EC was used as a plasticizer. The stainless steel (SS) blocking electrode was used in the

* Corresponding author. Tel./fax: +86-431-568-9711.
E-mail address: dongsj@ns.ciac.jl.cn (S. Dong).

0254-0584/02/$ – see front matter
PII: S0254-0584(01)00408-4

impedance experiments. In an attempt to study the effects of the plasticizer on conductivity, the impedance experiments were conducted using the plasticized SPE with different EC concentration in the temperature range 20–100 °C.

2. Experimental

PEO ($M_w = 5\times10^5$), EC and $LiClO_4$, each from Aldrich, were used. PEO and $LiClO_4$ were dried in a vacuum oven for 48 h at 50 °C and 72 h at 120 °C, respectively. Acetonitrile (Beijing Chemical Plant) was dried by addition of 4 Å type molecular sieves before use.

The SPE samples were prepared according to the procedure described elsewhere [26]. The concentration of $LiClO_4$ in the samples can be expressed as O:Li = 16:1, where O:Li is the mole ratio of polymer ether repeat unit to salt cation. This is the optimum value as was described previously by Angell et al. [27]. While the amount of EC, w_t% was calculated by the following equation:

$$w_t\% = \frac{W_{EC}}{W_{EC} + W_{PEO} + W_{salt}} \quad (1)$$

where W_{EC}, W_{PEO}, and W_{salt} is the weight of EC, PEO, and $LiClO_4$, respectively. The solid components were mixed in appropriate amounts in a small glass reactor, and then acetonitrile was added to form about 5 mass% suspension. The mixture was stirred magnetically until a homogeneous suspension was obtained. For the SPE thin films, the suspensions obtained were dropped into a home-build cell, which was shown in Fig. 1a, then left it to evaporate the solvent slowly at room temperature. The resulted films were then dried in a vacuum oven at 30 °C for 48 h before transferring to an argon-filled tube with anhydrous P_2O_5.

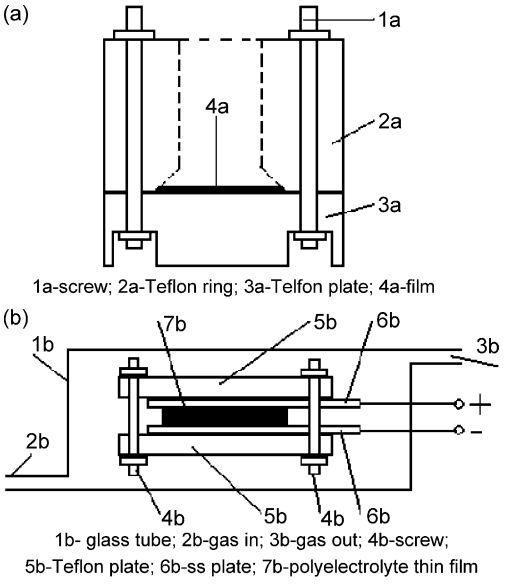

Fig. 1. (a) A schematic of the cell for the preparation of SPE thin films. (b) The cell for AC impedance experiments.

Differential scanning calorimetry (DSC) was carried out using Perkin-Elmer-7 system with a heating rate of 10 K min^{-1} from −60 to 100 °C.

Impedance measurements were carried out on a Solartron 1250 frequency analyzer coupled to 1286 electrochemistry-interface over the frequency range 1–65 535 Hz. The SPE film was cut to a required size and then was sandwiched between SS blocking electrodes. The experiment cell for impedance measurements is shown in Fig. 1b. An AC perturbation of 50 mV and DC potential of 100 mV were applied. The cell was kept in a temperature-controlled oven with a flow of dry N_2. Before performing each impedance measurement, the cell was kept at the testing temperature for at least 30 min to allow the thermal equilibration.

3. Results and discussion

3.1. Impedance spectra of $(PEO)_{16}LiClO_4$/EC

Impedance spectra are useful not only in determining the appropriate equivalent circuit and estimating the values of the circuit parameters, but also in analyzing the properties of SPE/electrode interface. Fig. 2 shows the impedance spectra of $(PEO)_{16}LiClO_4$/EC films with SS symmetrical blocking electrodes at room temperature. The impedance spectra of $(PEO)_{16}LiClO_4$ (SPE without EC) are also given in Fig. 2A (curve a). In the Nyquist plot (Fig. 2A) which is similar to that reported in the literature [28], there is a compressed semicircle in high frequency range and a straight line in the low frequency range for $(PEO)_{16}LiClO_4$ and $(PEO)_{16}LiClO_4$/EC, respectively. But when EC concentration reaches 20%, the semicircle disappears in high frequency range, which may be ascribed to the limit of measurable frequency of the instrument [2].

In Fig. 2A, the decrease of diameter of the semicircle in high frequency and the intercept of the straight line on real part axis with the increasing of EC concentration can be seen. When EC concentration is above 20%, the difference of the intercept between two straight lines becomes smaller, but the trend can be seen clearly in Fig. 2B. In Fig. 2B, the frequency-independent horizontal line roughly gives the bulk resistance. Another interesting phenomena in Fig. 2A is that the slope of the straight line is decreased especially from $(PEO)_{16}LiClO_4$ to $(PEO)_{16}LiClO_4$/EC samples, which may be caused by the roughness of SPE/electrode interface.

As reported previously, the equivalent circuit is an efficient method to interpret the complex impedance spectra [29–31]. According to the results described above, an equivalent circuit was proposed and it is shown in the inset of Fig. 2A, in which two constant phase elements (CPEs) have been used instead of the geometrical capacitance and double layer capacitance. CPE_1 represents the characteristics of the

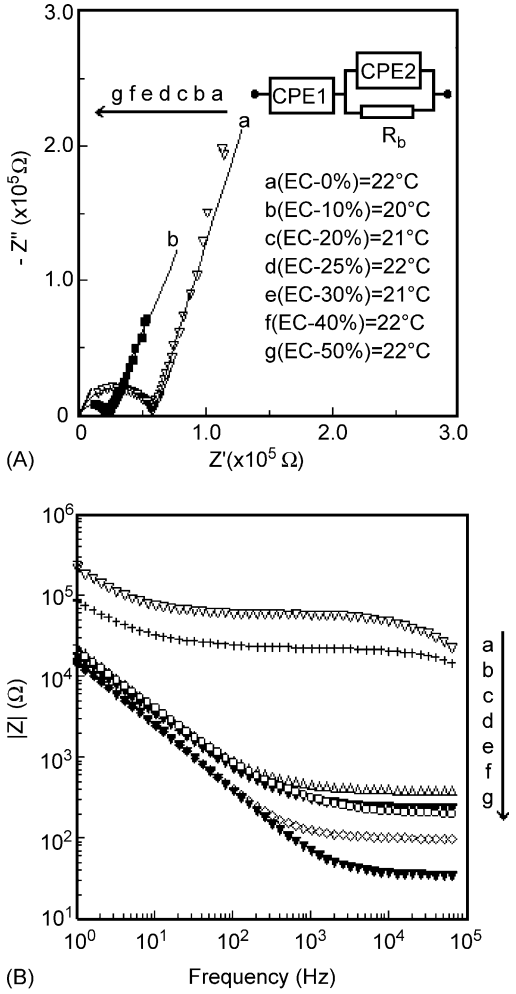

Fig. 2. Impedance spectra of $(PEO)_{16}LiClO_4$/EC films with SS symmetrical blocking electrodes at room temperature.

double layer between electrolyte/electrode interface, CPE_2 the SPE bulk properties and the effects of dipolar relaxation [32]. The high frequency semicircle reflects from the combination of R_b and CPE_2, while the straight line after the semicircle arising can be explained with CPE_1 corresponding to the double layer capacity of an in-homogeneous electrode surface. In the analyzing of CPE, impedance Z_{CPE} can be expressed as following:

$$Z_{CPE} = A(j\omega)^{-n} \tag{2}$$

$$\alpha = (1-n)\frac{\pi}{2} \tag{3}$$

where A is the inverse of the capacitance and n is related to α (the deviation from the vertical line in Nyquist plot); $n = 1$ indicates a perfect capacitance, and the lower n value directly reflects the roughness of the electrode used [33].

In the software used in this paper, the CPE is defined by two parameters CPE-T and CPE-P. CPE-T indicates the value of capacitance of CPE element, while CPE_1-P is a parameter indicates the slope of the low frequency straight line and CPE_2-P indicates the changes of compressed semicircle from an ideal semicircle. CPE-P is a parameter that equals n in Eqs. (2) and (3). Using the equivalent circuit, the impedance spectra in Fig. 2A can be analyzed by superimposing the best fit of the dispersion data. The estimated values together with the results of DSC are summarized in Table 1. The fitted results (solid line shown in Fig. 2A (a and b)) show the assumed equivalent circuit fits the experimental impedance data very well. The resistance determined is used to obtain the ionic conductivity by the following equation:

$$\delta = \frac{1}{R_b}\frac{d}{S} \tag{4}$$

where δ is the ionic conductivity, d the thickness of the SPE thin film, and S the area of SS electrode contacting with the SPE film.

From the data listed in Table 1, it can be seen clearly that δ increases with the increase of EC concentration. Moreover, the parameters of CEP_1-P firstly decrease with increasing of EC concentration up to 25%, and then almost reach constant, which can be used to explain the change of the straight line in the low frequency range. The decreased CEP_1-P value will make α increasing from Eq. (3). For the plasticized SPE at low EC concentration (lower than 25%), the decreased CPE_1-P indicates the roughness between SPE/electrode interface developed. When the EC concentration further

Table 1
Some parameters estimated from Fig. 2A using the equivalent circuit and the results of DSC measurement

Sample $[(PEO)_{16}–LiClO_4–x\text{-EC}]$	Fitted parameters						DSC results		
	CPE_1-T ($\times10^{-5}$)	CPE_1-P	CPE_2–T ($\times10^{-9}$)	CPE_2-P	R_b (Ω)	δ ($\times10^{-6}\,\Omega^{-1}\,cm^{-1}$)	T_g (°C)	X_c (%)	d/S (cm^{-1})
$x = 0\%$	0.114	0.797	1.15	0.78	57474	0.13	−49.89	37.10	0.0075
$x = 10\%$	0.360	0.689	1.80	0.77	22382	0.89	−53.85	32.80	0.0200
$x = 20\%$	1.100	0.756	1.60	0.77	414.1	29.00	−57.02	30.20	0.0120
$x = 25\%$	1.500	0.745	1.70	0.77	228.97	40.20	−59.52	27.48	0.0092
$x = 30\%$	1.600	0.745	1.40	0.77	143.23	69.80	−60.60	30.04	0.0100
$x = 40\%$	1.750	0.750	2.00	0.77	97.08	267.80	−59.88	21.30	0.0260
$x = 50\%$	2.500	0.750	1.00	0.77	33.90	236.00	−58.33	16.50	0.0080

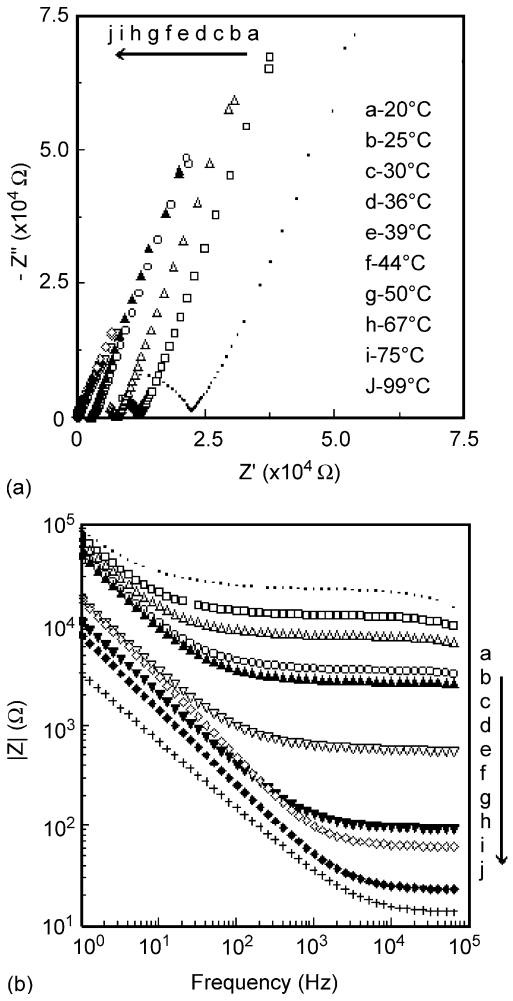

Fig. 3. Impedance spectra of $(PEO)_{16}LiClO_4$/EC(10%) films with SS symmetrical blocking electrodes at different temperatures.

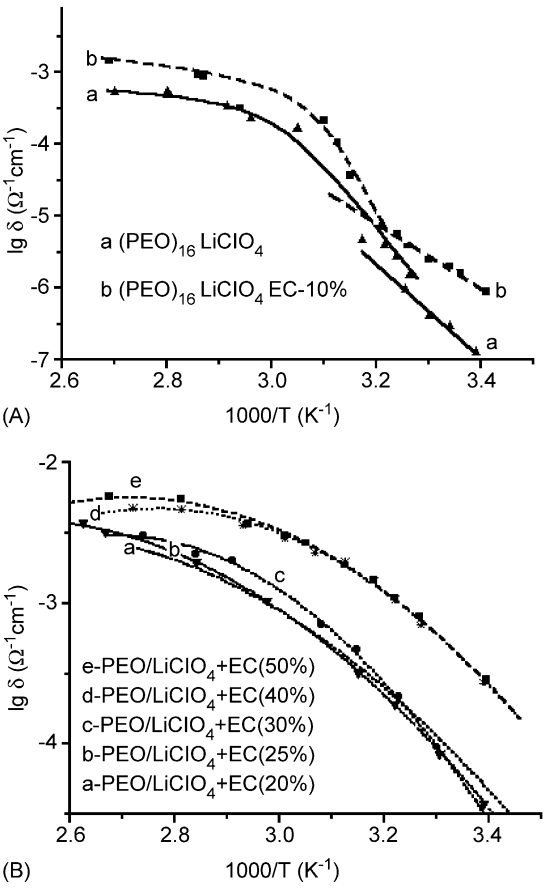

Fig. 4. Plots of $\log(\delta T)$ vs. 1000/T for the system $(PEO)_{16}LiClO_4$–*x*-EC. (A) Values of *x* are: (a) 0; (b) 10%. (B) Values of *x* are: (a) 20; (b) 25; (c) 30; (d) 40; (e) 50%.

increases, the constant CPE_1-P value suggests a homogeneous SPE being formed, which will lead to a good contact between SPE and SS electrode [34].

Fig. 3 shows the impedance spectra of $(PEO)_{16}LiClO_4$/EC(10%) at different temperatures. It is clear that the diameter of the semicircle in high frequency decreases with the increase of the experiment temperature and the semicircle in high frequency vanishes at the temperature above 35 °C. On the other hand, the slope of the straight line in low frequency does not tend to vary as a function of temperature which is similar to $PEO/Mg(CF_3SO_3)_2$ system observed by Morales and Acosta [35]. The change of the diameter of the semicircle indicates that R_b decreases with the increase of temperature. At high temperature, the frequency range required for the appearance of the semicircle should be higher than 100 kHz [36], but in our experiment 100 kHz is beyond the limitation of the measuring instrument. In such a case, ionic conductivity can be calculated from R_b value obtained from the estimation using the equivalent circuit inserted in Fig. 2A.

3.2. Ionic conductivity and its temperature dependence

It is well known that the conductivity of SPE depends strongly on the temperature. The ionic conductivity of plasticized $(PEO)_{16}LiClO_4$/EC samples containing various amounts of EC as a function of temperature is shown in Fig. 4. From Fig. 4, several features can be observed:

1. In the temperature range studied, the conductivity is found to increase with temperature for all the $(PEO)_{16}LiClO_4$/EC samples.
2. The room temperature conductivities increase with increase of EC concentration. For sample containing 40% EC, the room temperature conductivity is four orders of magnitude larger than that of $(PEO)_{16}LiClO_4$ sample.
3. For $(PEO)_{16}LiClO_4$ and $(PEO)_{16}LiClO_4$/EC(10%) samples (Fig. 4A), the conductivity–temperature plots have two obvious regions, i.e. Li^+ transport properties are controlled by two distinct mechanisms. In low temperature region, the conductivity increases with temperature up to 65 °C which corresponds to the melting point (66 °C) of PEO [37]. The linear relationship reveals that the temperature dependence of conductivity

follows Arrhenius form, suggesting that the conductivity is thermally activated. At 65 °C, there is a sudden increase in conductivity. While in the high temperature region, the conductivity again increases with temperature. The temperature dependence of conductivity follows VTF empirical form, i.e. the migration of lithium cations depends mainly on the segmental movements of the polymer chain in the amorphous region. Similar behavior has been observed for PEO/$LiClO_4$ [37] and PEO–poly(*N*,*N*-dimethylacrylamide (NNPAAM))–$LiClO_4$ [26] systems.

4. For the samples with EC concentration above 20%, the temperature dependence of conductivity follows VTF behavior throughout.

The Arrhenius type and VTF empirical form can be expressed as

$$\delta = \delta_0 \exp\left(\frac{-E_a}{RT}\right) \tag{5}$$

$$\delta = \frac{A}{T^{1/2}} \exp\left(\frac{-E_b}{K(T - T_0)}\right) \tag{6}$$

where δ_0 and A is the conductivity pre-exponential factor, and E_a and E_b the activation energy of ionic conduction for Eqs. (5) and (6), respectively. T_0 is the thermodynamic glass transition temperature which is usually 50 K lower than the glass transition temperature (T_g) [38]. K is the Boltzmann constant. The VTF plots of $\log(\delta T^{1/2})$ vs. reciprocal $(T - T_0)$ for $(PEO)_{16}LiClO_4$/*x*-EC with $x = 20$, 30, 35, 40, and 50% were shown in Fig. 5. The straight lines indicate clearly that the temperature dependence of conductivity obeys the VTF relationship.

The enhanced ionic conductivity of the plasticized SPE can be understood by the interactions among PEO, EC, and $LiClO_4$. The oxygen of C=O in EC is an electron donor which can enter in competition with ClO_4^- and PEO. The interactions can be summarized as follows: ion–ion interaction between Li^+ cations and ClO_4^- anions; ion–dipole interactions between Li^+ cations and carbonyl oxygens in PEO; ion–molecule interactions between Li^+ and EC. The Li^+–EC interactions include not only between Li^+ and oxygen atoms of the C=O group, but also between Li^+ and another two oxygen atoms in the ring structure of EC [39]. These interactions are of importance to form PEO–$LiClO_4$–EC polymeric electrolyte, in which three different compounds of PEO–Li^+, PEO–Li^+–EC, and Li^+–EC exist.

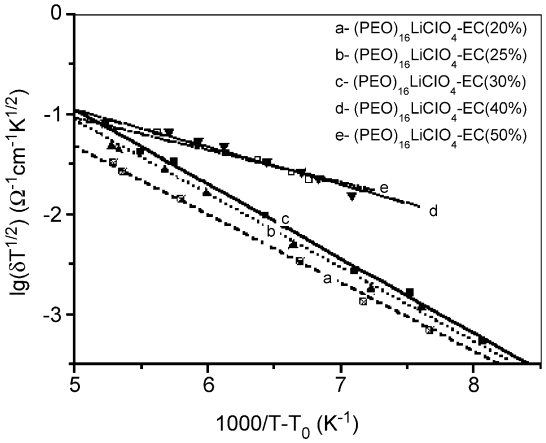

Fig. 5. VTF plots of $\log(\delta T^{1/2})$ vs. reciprocal $(T - T_0)$ for the system $(PEO)_{16}LiClO_4$–*x*-EC. Values of *x* are: (a) 20; (b) 25; (c) 30; (d) 40; (e) 50%.

To understand the effect of EC on the conductivity of $(PEO)_{16}LiClO_4$/EC system, the Li^+–EC interaction seems critical. The addition of EC initially leads to the formation of Li^+–EC complex, which will reduce the fraction of PEO–Li^+ complex and increase the flexibility of PEO chains. The increase in flexibility is reflected in a decrease in T_g, which is the reason why the room temperature conductivity increases with the addition of EC plasticizer. Although the competition interactions among PEO, Li^+, and EC exist, the Li^+–EC interaction is weaker than PEO–Li^+. It is to say that EC is not a good competitor against PEO for complex formation with Li^+ cation [24]. At low EC concentration, there is a little effect on the fraction of PEO–Li^+ complex. The thermal activation still dominates the ionic conductivity at low temperature, whereas at high temperature the transport of ions is coupled to the segmental motion of the polymeric chains. With the further increase of EC, PEO–Li^+–EC complex increases until to a saturation level. During this stage, Li^+ ion may prefer to conduct through these new paths because the medium is less viscous, thus enhancing mobility of ion [40]. Under this situation, the ionic transport depend on the motions of the coupling of charge carries with the polymeric segments, and the temperature dependence conductivity follows the VTF type behavior.

4. Conclusion

The effects of plasticizer EC for $(PEO)_{16}LiClO_4$/EC system are analyzed in two aspects. The first is focused on the AC impedance spectra. With the increase of EC concentration, the semicircle in high frequency range vanishes and at the beginning of the addition of EC the slope of the straight line in low frequency decreases. The change of the semicircle in high frequency range is due to the limitation of the experiment instrument, but the decrease of the straight line in low frequency range is attributed to the characteristics of electrolyte/electrode interface. The experiment data can be interpreted using an equivalent circuit proposed.

The second is the enhanced ionic conductivity. The temperature-dependence conductivity plots in high temperature range show the VTF behavior, but in the low temperature range the plots change to VTF form from the Arrhenius behavior with increasing of EC concentration. In $(PEO)_{16}LiClO_4$/EC system, the interactions among Li^+–ClO_4^-, Li^+–PEO, and Li^+–EC will cause three

different compounds such as PEO–Li^+, PEO–Li^+–EC, and Li^+–EC. At low EC concentration, the fraction of PEO–Li^+ changes a little, the ion conduction is almost the same as that without EC plasticizer. While at high EC concentration, the formation of PEO–Li^+–EC will create a new path for the transport of Li^+ ion, which increases the ionic conductivity.

Acknowledgements

Financial supports from National Nature Science Foundation of China (No. 20075028), K.C. Wang Post-doctoral Research Award Fund of Chinese Academy of Sciences and China Post-doctoral Science Foundation are acknowledged.

References

[1] M. Watanabe, H. Uchida, M. Emori, J. Phys. Chem. B 102 (1998) 3129.
[2] H.Y. Sung, Y.Y. Wang, C.C. Wan, J. Electrochem. Soc. 145 (1998) 1207.
[3] M.A.K.L. Dissanayake, R. Frech, Macromolecules 28 (1995) 5312.
[4] P. Lightfoot, M.A. Mehta, P.G. Bruce, Science 262 (1993) 883.
[5] W. Xu, Z.H. Deng, X.Z. Zhang, G.X. Wan, J. Solid State Electrochem. 2 (1998) 257.
[6] W. Wieczorek, D. Raducha, A. Zalewska, J.R. Stevens, J. Phys. Chem. B 102 (1998) 8725.
[7] P.P. Chu, H.P. Jen, F.R. Lo, C.L. Lang, Macromolecules 32 (1999) 4738.
[8] D. Fenton, J.M. Parker, P.V. Wright, Polymer 14 (1973) 589.
[9] P.P. Prosini, T. Fujieda, S. Passerini, M. Shikano, T. Sakai, Electrochem. Commun. 2 (2000) 44.
[10] P.G. Bruce, C.A. Vincent, J. Chem. Soc. Faraday Trans. 89 (1993) 3187.
[11] P.V. Wright, Electrochim. Acta 43 (1998) 1137.
[12] W.H. Meyer, Adv. Mater. 10 (1998) 439.
[13] D. Baril, C. Michot, M. Armand, Solid State Ionics 94 (1997) 35.
[14] K. Murata, S. Izuchi, Y. Yoshihisa, Electrochim. Acta 45 (2000) 1501.
[15] H.S. Choe, B.G. Carroll, D.M. Pasquariello, K.M. Abraham, Chem. Mater. 9 (1997) 369.
[16] C. Vachon, C. Labreche, A. Vallee, S. Besner, M. Dumont, J. Prud'homme, Macromolecules 28 (1995) 5585.
[17] H.J. Rhoo, H.T. Kim, J.K. Park, T.S. Hwang, Electrochim. Acta 42 (1997) 1571.
[18] Z. Florjunczyk, W. Bzducha, W. Wieczorek, E.Z. Monikowska, W. Krawiec, S.H. Chung, J. Phys. Chem. B 102 (1998) 8409.
[19] H.S. Lee, X.Q. Yang, J. McBreen, Z.S. Xu, T.A. Skotheim, Y. Okamoto, J. Electrochem. Soc. 141 (1994) 886.
[20] J.Y. Kim, S.H. Kim, Solid State Ionics 124 (1999) 91.
[21] D.G.H. Ballard, P. Cheshire, T.S. Mann, J.E. Przeworski, Macromolecules 23 (1990) 1256.
[22] K.H. Lee, J.K. Park, W.J. Kim, J. Polym. Sci. B 37 (1999) 247.
[23] W.T. Whang, C.L. Lu, J. Appl. Polym. Sci. 56 (1995) 1635.
[24] T. Li, P.B. Balbuena, J. Electrochem. Soc. 146 (1999) 3613.
[25] T.T. Cheng, T.C. Wen, J. Electroanal. Chem. 459 (1998) 99.
[26] W. Wieczorek, A. Zalewska, D. Raducha, Z. Florjanczyk, J.R. Stevens, A. Ferry, P. Jacobsson, Macromolecules 29 (1996) 143.
[27] C.A. Angell, C. Liu, E. Sanchez, Nature 362 (1993) 137.
[28] M.L.G. Mancini, L. Honeycutt, D. Teeters, Electrochim. Acta 45 (2000) 1491.
[29] X.M. Qian, N.Y. Gu, Z.L. Cheng, X.R. Yang, E.K. Wang, S.J. Dong, J. Solid State Electrochem. 5 (2001), in press.
[30] X.M. Ren, P.G. Pickup, J. Electroanal. Chem. 420 (1997) 251.
[31] M. Watanabe, K. Sanui, N. Ogata, J. Appl. Phys. 57 (1985) 123.
[32] X.M. Qian, N.Y. Gu, Z.L. Cheng, X.R. Yang, E.K. Wang, S.J. Dong, Electrochim. Acta 46 (2001) 1829.
[33] J.M. Zen, G. Ilangovan, J.J. Jou, Anal. Chem. 71 (1999) 2797.
[34] X.M. Qian, N.Y. Gu, Z.L. Cheng, X.R. Yang, E.K. Wang, S.J. Dong, J. Graduate School, Acad. Sin. 17 (2) (2000) 39 (in Chinese).
[35] J.L. Morales, E. Acosta, Electrochim. Acta 43 (1998) 791.
[36] N. Munichandraiah, L.G. Scanlon, R.A. Marsh, B. Kumar, A.K. Sircar, J. Appl. Electrochem. 25 (1995) 857.
[37] T. Sreekanth, M.J. Reddy, S. Subramanyam, U.V. Subba Rao, Mater. Sci. Eng. B 64 (1999) 107.
[38] V. Munchow, V. Di Noto, E. Tondello, Electrochim. Acta 45 (2000) 1211.
[39] Z. Wang, B. Huang, R. Xue, L. Chen, F. Wang, J. Electrochem. Soc. 143 (1996) 1510.
[40] L.R.A.K. Bandara, M.A.K.L. Dissanayake, B.E. Mellander, Electrochim. Acta 43 (1998) 1447.